Bilayer Hydrogel With Autologous Stem Cells Derived From Debrided Human Burn Skin for Improved Skin Regeneration

Shanmugasundaram Natesan, PhD, David O. Zamora, PhD, Nicole L. Wrice, BS, David G. Baer, PhD, Robert J. Christy, PhD

The objective of this study was to demonstrate that stem cells isolated from discarded skin obtained after debridement can be used with collagen and fibrin-based scaffolds to develop a tissue-engineered vascularized dermal equivalent. Discarded tissue samples were collected from severely burned patients undergoing wound debridement. Stem cells were isolated from the adipose tissue layer and their growth and immunophenotype characterized. To develop a skin equivalent, debrided skin adipose stem cells (dsASCs) were added to a collagen-polyethylene glycol (PEG) fibrin-based bilayer hydrogel and analyzed in vitro. The effect of the bilayered hydrogels on wound healing was demonstrated using an excision wound model in athymic rats. The dsASCs isolated from all samples were CD90, CD105, and stromal cell surface protein-1 positive, similar to adipose stem cells isolated from normal human lipoaspirates. Within the bilayer hydrogels, dsASCs proliferated and differentiated, maintained a spindle-shaped morphology in collagen, and developed a tubular microvascular network in the PEGylated fibrin. Rat excision wounds treated with bilayer hydrogels showed less wound contraction and exhibited better dermal matrix deposition and epithelial margin progression than controls. Stem cells can be isolated from the adipose layer of burned skin obtained during debridement. When dsASCs are incorporated within collagen-PEGylated fibrin bilayer hydrogels, they develop stromal and vascular phenotypes through matrix-directed differentiation without use of growth factors. Preliminary in vivo studies indicate that dsASC-bilayer hydrogels contribute significantly to wound healing and provide support for their use as a vascularized dermal substitute for skin regeneration to treat large surface area burns. (J Burn Care Res 2013;34:18–30)

Burn wounds constitute 5 to 10% of military casualties, often involving 40 to 60% of total body surface area (TBSA).[1–3] Combat injuries are unique as most of the burn wounds are often associated with other traumatic extremity injuries and therefore require additional surgical procedures over the treatment of the primary burn wounds.[4,5] Analysis of differences between civilian and military burn victims treated in the same facility showed a similar distribution of total burn size at approximately 15% TBSA across both populations. However, the percentage TBSA that had full-thickness burns was significantly higher in the military than in the civilian populations.[3,6] Normally, treatment of these wounds involves multiple skin-grafting surgeries using autologous skin. Unfortunately, large surface burn wounds lack autologous viable uninjured tissue for grafting, making them extremely difficult for the burn surgeon to treat, manage, and reconstruct the wounds.

When autograft skin is unavailable, these extensive wounds are treated with allogeneic decellularized

1. REPORT DATE	2. REPORT TYPE	3. DATES COVERED
01 JAN 2013	**N/A**	**-**

4. TITLE AND SUBTITLE	5a. CONTRACT NUMBER
Bilayer Hydrogel With Autologous Stem Cells Derived From Debrided Human Burn Skin for Improved Skin Regeneration.	5b. GRANT NUMBER
	5c. PROGRAM ELEMENT NUMBER

6. AUTHOR(S)	5d. PROJECT NUMBER
Natesan S., Zamora D. O., Wrice N. L., Baer D. G., Christy R. J.,	5e. TASK NUMBER
	5f. WORK UNIT NUMBER

7. PERFORMING ORGANIZATION NAME(S) AND ADDRESS(ES)	8. PERFORMING ORGANIZATION REPORT NUMBER
United States Army Institute of Surgical Research, JBSA Fort Sam Houston, TX	

9. SPONSORING/MONITORING AGENCY NAME(S) AND ADDRESS(ES)	10. SPONSOR/MONITOR'S ACRONYM(S)
	11. SPONSOR/MONITOR'S REPORT NUMBER(S)

12. DISTRIBUTION/AVAILABILITY STATEMENT
Approved for public release, distribution unlimited

13. SUPPLEMENTARY NOTES

14. ABSTRACT

15. SUBJECT TERMS

16. SECURITY CLASSIFICATION OF:			17. LIMITATION OF ABSTRACT	18. NUMBER OF PAGES	19a. NAME OF RESPONSIBLE PERSON
a. REPORT **unclassified**	b. ABSTRACT **unclassified**	c. THIS PAGE **unclassified**	**UU**	**13**	

skin or tissue-engineered substitutes containing allogeneic and/or autologous cells. These tissue-engineered wound dressings have resulted in the emergence of a range of dermal, epidermal, and even complete skin equivalents and include Apligraf® (Organogenesis, Canton, MA), Dermagraft® (Advanced Tissue Sciences, La Jolla, CA), and Epicel® (Genzyme Biosurgery, Cambridge, MA).[7–9] Although these products have proven useful in a wide variety of wound care applications, significant challenges remain, including the availability of autologous cells, the time required for culture expansion from a biopsy, and failure of graft integration because of poor vascularization. Moreover, normal tissue accessibility proportionally decreases with percentage increase in TBSA.[10] Therefore, therapies for severely burned patients will require an alternative source of tissue and cells to develop a tissue-engineered skin construct that has better engraftment results. Recent reports show that stem cells from bone marrow[11,12] or adipose tissue[13–15] improve the wound healing process either through direct cellular interaction or through paracrine effects. Adipose-derived stem cells (ASCs), in particular, can be obtained in abundance with a minimally invasive liposuction technique.[16,17] Unfortunately, after severe burn injury, the sources of adipose tissue are limited primarily because of the unavailability of viable tissue and limited clinical access to normal sources of adipose tissue (eg, subcutaneous lipoaspirate). Recently, we have shown that stem cells can be isolated in good quantities from the adipose layer of discarded burned skin (dsASCs) obtained during surgical debridement of necrotic tissue associated with a burn eschar. Further, these cells were able to integrate within the excision wound bed of an athymic rat.[18] The dsASCs can be isolated proportionally in large numbers from patients with increasing percentage TBSA burn and can be used to develop tissue-engineered treatment options for wound healing and skin reconstruction.

It is extremely important in creating a suitable microenvironment for stem cells to survive and participate in regeneration and repair of a burn wound.[19–22] Recent studies have shown that natural biomaterial-based scaffolds, such as collagen, alginate, hyaluronic acid, fibrin, and chitosan, provide a favorable microenvironment for stem cells to maintain a balance between self-renewal and differentiation in situ.[9,23–25] This study demonstrates that dsASCs isolated from discarded burned skin obtained after debridement can be used along with collagen and fibrin-based scaffolds to develop a tissue-engineered vascularized dermal equivalent. Further, it demonstrates the effectiveness of the tissue-engineered construct using an excision wound model in athymic rats.

METHODS

Skin Samples From Debrided Burn and Human Abdominoplasty

Discarded skin from patients undergoing burn wound debridement and normal skin and adipose tissue from patients undergoing abdominoplasty were obtained from the U.S. Army Institute of Surgical Research Burn Center and Brooke Army Medical Center, Fort Sam Houston, Texas, respectively. The samples were brought to the laboratory immediately after debridement or abdominoplasty procedures. Before the debrided tissue was processed, 5 mm diameter punch biopsies were taken from different areas of the burned skin and fixed in 10% buffered formalin for histological analysis. This study was conducted under the protocol reviewed and approved by the U.S. Army Medical Research and Materiel Command Institutional Review Board. Discarded burn tissue samples and skin tissue from patients undergoing abdominoplasty were collected in accordance with the approved protocols, HSC20080290N and H-11–020, respectively.

Histological Analysis

Histological analysis was performed using 10% buffered formalin-fixed biopsies. The fixed samples were processed and embedded in paraffin, and 5- to 7-μm sections were cut and stained with Masson's trichrome stain (MTS). Stained sections of the discarded human skin biopsies were used to assess tissue viability and burn depth, and an abdominoplasty procedure skin sample was used as a control. The granulated skin tissue from the athymic rats treated with bilayer hydrogels, (PEGylated fibrin-collagen)–dsASCs bilayer hydrogels, and saline controls were collected on days 8 and 16 to determine the overall wound healing pattern.

Isolation and Culture of Adipose-Derived Stem Cells

Stem cells from skin samples obtained after burn wound debridement and abdominoplasty were isolated as previously described.[18] The authors were blinded from some patient information including burn depth, percentage TBSA, and anatomical location of the burn. Briefly, the skin samples were washed 3 to 4 times with Hank's buffered salt solution (HBSS) to remove adherent blood clots.

The hypodermal layer was dissected away from the dermal region, transferred to a petri dish, and finely minced with scissors. The minced tissue was suspended in HBSS and centrifuged for 10 minutes at $500g$ at 16°C. The floating tissue was carefully collected, and to every 1 ml of the floating fraction tissue, 3500 units of collagenase type II (Sigma-Aldrich, St. Louis, MO) was added and incubated for 45 to 60 minutes at 37°C in an orbital shaker incubator at 125 rpm. The undigested tissue was removed by sequential passage through 100- and 70-μm nylon mesh filters. The filtrate was then centrifuged at $500g$ for 10 minutes at 16°C, treated with BD Pharm Lyse™ lysing buffer (BD Bioscience, San Jose, CA) to remove any remaining red blood cells, and washed twice with HBSS. The final cell pellets were resuspended in growth media (Mesen-PRO RS™ basal medium), supplemented with MesenPRO RS™ growth supplement, antibiotic–antimycotic (100 U/ml of penicillin G, 100 μg/ml streptomycin sulfate, and 0.25 μg/ml amphotericin B), and 2 mM of L-glutamine (Life Technologies, Carlsbad, CA). The resulting cells ($\approx 1.7 \times 10^6$) were cultured in T75 flasks (BD Falcon, NJ) and maintained in a 5% CO_2 humidified incubator at 37°C. After 4 hours in culture, the growth medium was replaced to remove any floating debris. The remaining attached cells from abdominoplasty were designated as ASCs and cells from debrided skin as dsASCs. The capacity of dsASCs to proliferate from samples obtained from different age groups—young (21 years; BH1), middle age (49 years; BH2), and old (76 years; BH3)—was assessed by counting the number of cells every 48 hours. After counting, 6×10^3 cells/cm² were replated, and the process was repeated for eight consecutive passages.

To determine the proliferation rate of stem cells isolated from abdominoplasty and debrided skin samples, a viability assay using 3-(4,5-dimethylthiozole-2-yl)-2,5-diphenyltetrazolium bromide (MTT, Sigma-Aldrich, St. Louis, MO) was performed.[26] Briefly, passage 2 ASCs and dsASCs were seeded in a 12-well plate (5000 cells/well, n = 3) and growth media was removed and 25 μl of MTT solution (5 mg/ml) was added to each well and incubated for 4 hours in a 5% CO_2 humidified incubator at 37°C. After incubation, the MTT solution was removed and 250 μl of dimethyl sulfoxide (Sigma-Aldrich, St. Louis, MO) was added. The dissolved formazan complex from each well was collected, and absorbance was measured at 570 nm with 630 nm as reference and dimethyl sulfoxide as reagent blank using Molecular Devices Spectramax M2 Microplate Reader (Molecular Devices, Sunnyvale, CA).

Immunocytochemistry and Fluorescence-Activated Cell Sorting Analysis of dsASCs

Immunocytochemistry. Immunocytochemistry was performed on P1 cells isolated from patient BH2 and cultured on a two-well chambered slide (20,000 cells/well, Nalgene Nunc, LabTek® chamber slide, Naperville, IL) for 48 hours in a 5% CO_2 humidified incubator at 37°C. The cells were washed twice with sterile HBSS, fixed with 4% paraformaldehyde for 20 minutes, and incubated overnight at 4°C with antihuman monoclonal antibodies targeted against endoglin (CD105; 40 μg/ml; R&D Systems, Minneapolis, MN), STRO-1 (20 μg/ml; R&D Systems), Thy-1 (CD90; 10 μg/ml; BD Bioscience, San Jose, CA), or platelet-derived growth factor receptor beta (PDGFRβ; 50 μg/ml; BD Bioscience, San Jose, CA). The slides were then washed twice (5 minutes total) with HBSS and incubated with either 5 μg/ml Alexa Fluor® 488 or Alexa Fluor® 594 labeled secondary antibodies of corresponding Ig class for 45 minutes at 4°C. The nuclei were stained with Hoechst 33342 (10 μg/ml; Life Technologies) for 20 minutes at room temperature. Nonspecific fluorescence was examined by using cell preparations or tissue sections preincubated with either control unlabeled antibodies or fluorophore-labeled secondary antibodies.

Fluorescence-Activated Cell Sorting Analysis. Passage 1 cells isolated from patient BH2 were analyzed for immunophenotype by flow cytometry fluorescence-activated cell sorting (FACS). Adherent cells were washed twice with HBSS, trypsinized, and resuspended in FACS cell-staining buffer (Biolegend, San Diego, CA) to a final concentration of 5×10^5 cells/100 μl. Cells were immunostained for cell surface markers by incubating them for 45 minutes with labeled primary mouse antihuman antibodies (5–10 μg/ml): CD90-phycoerythrin (PE), CD105-PE, STRO-1-Alexa Fluor® 647 (Biolegend), and CPDGFRβ-PE (BD Bioscience). Control cells were also incubated with their respective isotype controls IgG1-PE, IGg1-FITC, IgG_{2A}-PE, or IgM-Alexa Fluor® 647 (10 μg/ml). Cells were washed twice and then resuspended in 500 μl of cell-staining buffer. FACS analysis was performed using a FACS Aria flow cytometer (BD Biosciences). Before analysis, the forward scatter and the side scatter were adjusted for each sample using appropriate unstained cells to eliminate dead cells and cell debris. Autofluorescence signals were eliminated by adjusting the signal outputs from designated channels, and the sensitivity was adjusted to collect a gated population of cells. Total percentage of cells staining positive for an individual

marker from the gated population was determined. Results were quantified by FACS Diva software (BD Biosciences), and 20,000 events were collected and analyzed for the total population positive for specific cell surface markers.

Preparation of dsASCs-Hydrogels

Collagen Hydrogels. Passage 2 (P2) dsASCs (50,000 cells/ml of gel mixture) isolated from patient BH2 were trypsinized and mixed with type 1 collagen (5 mg/mL; Trevigen, Gaithersburg, MD) obtained from rat tail tendon, and was fibrillated by adjusting the pH to 6.8 to 7.0 using 100 ml of Dulbecco phosphate buffered saline and 23 ml of 1N sodium hydroxide, according to the manufacturer's instructions. The collagen-dsASCs mixture was added to a six-well culture insert and incubated for 30 minutes at 37°C to complete gelation.

PEGylated Fibrin Hydrogels. PEGylated fibrin hydrogels were prepared as previously described with slight modifications.[27,28] Succinimidyl glutarate modified polyethylene glycol (SG-PEG-SG, 3400 Da; NOF America Corporation, White Plains, NY) was added to fibrinogen (Sigma-Aldrich) in a 1:10 molar concentration ratio, SG-PEG-SG:fibrinogen, in tris-buffered saline, pH 7.8, and incubated for 20 minutes at 37°C. P2 dsASCs (50,000 cells/ml of hydrogel mixture) isolated from patient BH2 were added to PEG-fibrinogen mixture. To initiate gelation, an equal volume of thrombin (Sigma-Aldrich) in 40 mM of calcium chloride at a final concentration of 10 U/mL was added and incubated for 10 minutes at 37°C. The resulting hydrogel was then rinsed with tris-buffered saline to remove unbound SG-PEG-SG.

PEGylated Fibrin-Collagen Bilayer Hydrogels. The bilayer hydrogels were prepared as previously described[29] with slight modifications. Briefly, collagen-dsASCs hydrogels were prepared as described earlier. For the PEGylated fibrin hydrogels, thrombin was added to the PEGylated fibrinogen-dsASCs (50,000 cells/ml of hydrogel mixture), and the solution was carefully transferred to the top of the collagen-dsASCs hydrogel and allowed to gel completely.

The bilayer hydrogels were incubated with α minimal essential media supplemented with 10% fetal bovine serum, antibiotic–antimycotic (100 U/mL of penicillin G, 100 g/mL of streptomycin sulfate, 0.25 g/mL of amphotericin B, and 2 mM of L-glutamine [Life Technologies]) and maintained in a 5% CO_2 humidified incubator at 37°C. The stem cells within the hydrogels were observed for 10 days, and light microscopy pictures were taken at different

days with an Olympus IX71 inverted microscope equipped with a reflective fluorescence system.

In Vivo Analysis of PEGylated Fibrin-Collagen–dsASCs Bilayer Hydrogels in an Athymic Rat Full-Thickness Excision Wound Model. Male *rnu* nude rats (athymic rats), deficient in T-cell function, weighing 175 to 225 g were obtained from Harlan Laboratories (Indianapolis, IN) and housed in the animal care facility at the U.S. Army Institute of Surgical Research Burn Center with access to water and rat chow ad libitum. A full-thickness skin excision wound 1.5 cm in diameter was created on the dorsum of the rat down to the panniculus. Animals were randomly divided into three groups with eight rats per group; the saline control group (250 μl of saline), PEGylated fibrin-collagen bilayer group containing 1 ml of PEGylated fibrin and collagen bilayer hydrogels and a PEGylated fibrin-collagen–dsASCs bilayer group containing 1 ml of PEGylated fibrin and collagen bilayer gels and 50,000 cells in each hydrogel layer from patient BH1. All the wounds were covered with DuoDERM® dressing (ConvaTec, Skillman, NJ) and evaluated for 8 or 16 days. The wound bed for all animals was traced during the course of the study, and the wound area was calculated by using the number of pixels per square millimeter relative to control tracings at day 0 and the amount of healing expressed as percentage healing from day 0. The wound beds, including the margin of healed area surrounding the wound, were harvested on days 8 and 16. Samples were prepared for histology and stained with MTS as described earlier.

RESULTS

Adipose Tissue-Derived Stem Cells From Debrided Burn and Human Abdominoplasty

Skin samples obtained from a patient undergoing burn wound debridement or abdominoplasty procedures were brought to the laboratory and photographed. The hypodermal region of the skin sample obtained from patient human abdominoplasty (Figure 1A) shows the presence of a viable layer of adipose tissue with less necrosis, whereas the hypodermal region of debrided burned skin (Figure 1B) shows areas of tissue necrosis with blood clot and some viable adipose tissue layers. At the microscopic level, the MTS-stained section of the adipose tissue layer from abdominoplasty samples shows mature, round to polygonal adipocytes with clear cytoplasmic vacuoles (Figure 1C) separated with a thin line of interlobular septae arranged in a tight, mosaic-like pattern. MTS stained sections from burned skin
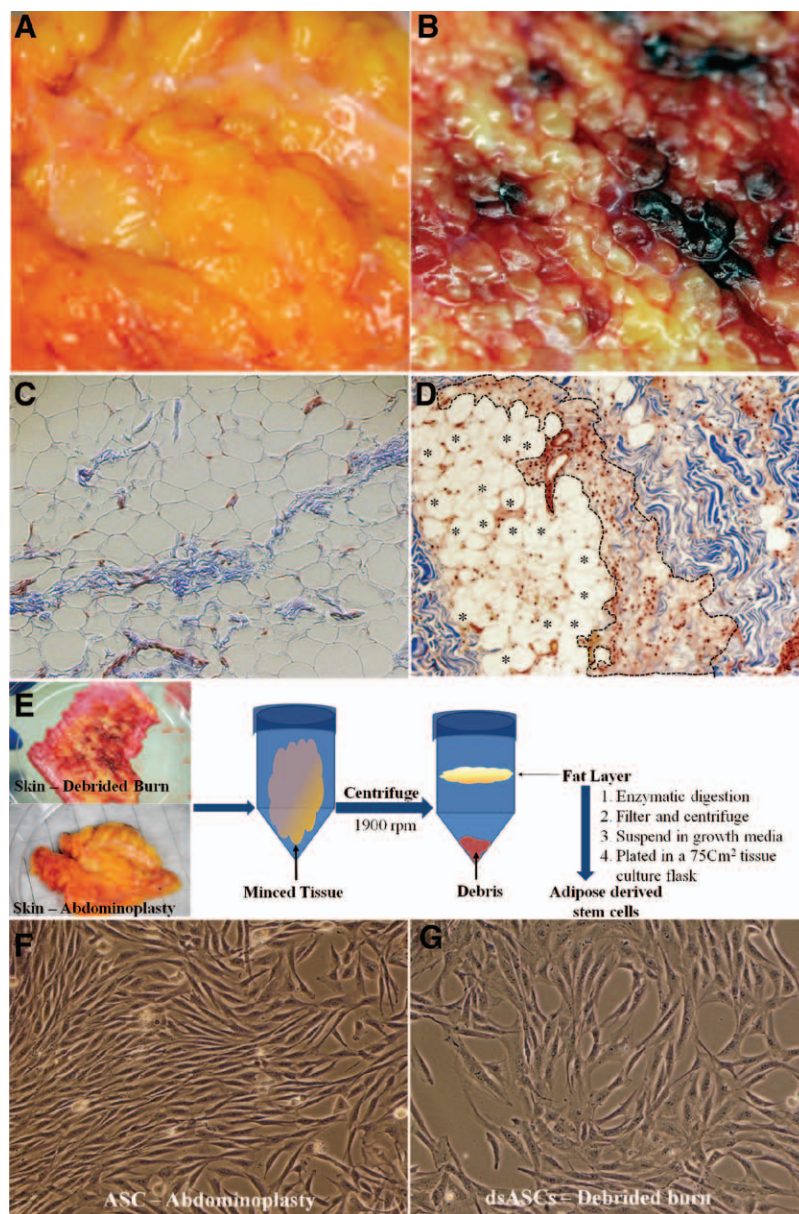
Figure 1. Photographic images of human adipose tissue obtained after (A) abdominoplasty, (B) burn wound debridement. Masson trichrome stained adipose tissue sections of (C) abdominoplasty adipose tissue showing the presence of an intact hypodermis and (D) discarded burn tissue showing both viable hypodermis (asterisks) and completely necrotized tissue (serrated line). E. Schematic representation showing stem cell isolation process from the adipose tissues of both debrided burn and abdominoplasty skin samples. Light micrograph images of passage 1 stem cells isolated from adipose tissue of (F) abdominoplasty and (G) discarded burn wound. Original magnification: ×100 (C, D) and ×200 (F, G).

samples (Figure 1D) show the presence of both partially intact (asterisk) and completely necrotized adipose tissue layer (region with serrated line) with granular cytoplasm and notable loss of clear vacuoles.

Adipose tissues of both debrided burn and abdominoplasty skin samples were processed using a similar protocol to obtain stem cells. Figure 1E shows the schematic representation of the cell isolation

procedure from adipose tissue. The cells isolated from the floating fraction after enzymatic digestion were plated; and after 4 hours, all the adherent cells were considered passage 0 (P0) and were supplied with fresh media. The cells derived from both debrided burn (Figure 1F) and human abdominoplasty (Figure 1G) adipose tissue layer exhibited characteristic fibroblast-like morphology with minimal gross morphological differences.

Patient Population and Stem Cell Proliferation

In the present study, dsASCs were isolated from samples obtained from patients varying in age from 15 to 90 (Figure 2A) with a mean age of 45 (n = 75).

Adherent dsASCs obtained from the floating hypodermal fraction from one of the youngest (17) and one of the oldest (76) patients were subjected to serial passages, and both showed a 3- to 4-fold increase in cell number every 48 hours up to P4 (Figure 2B).
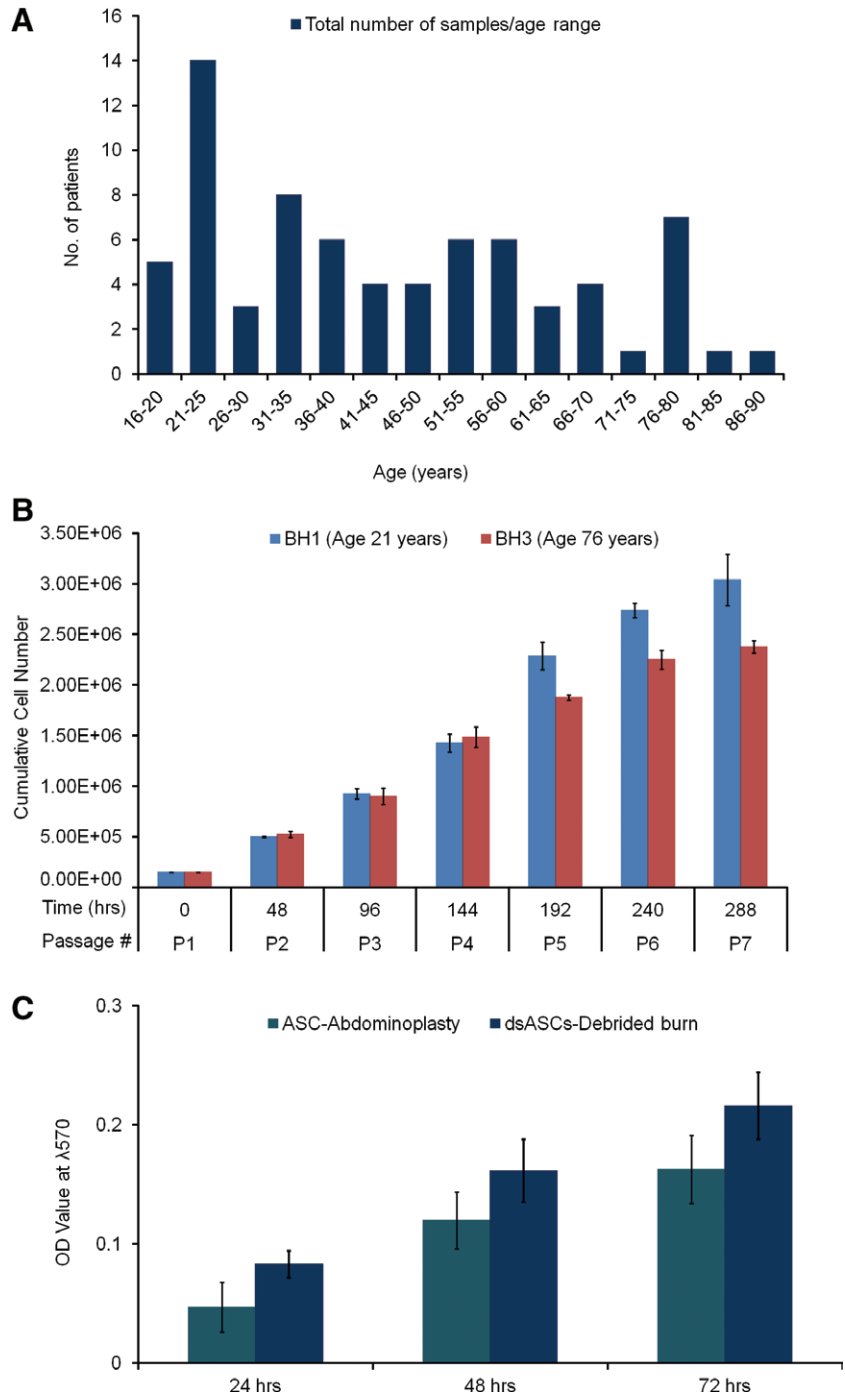

Figure 2. A. Bar graph representing total number of patient samples per age group included in this study. B. Comparative chart showing cumulative cell number of dsASCs serially passed with an initial seeding density of 6×10^3 cells/cm^2 surface area. BH1: isolated from a younger (21 years) patient and BH3: isolated from an older (76 years) patient. C. Bar graph representing proliferation of passage 2 adipose-derived stem cells islolated from abdominoplasty and debrided burn skin samples. OD, optical density.

After P4, dsASCs from the younger patient continued to show a consistent proliferation rate with minimal change/decrease in total cell number. On the contrary, in the dsASCs isolated from the sample the older burn patient showed a significant decrease in proliferation rate and total cell number at P5 having only a $< 2 \times 10^5$ cells per passage increase in cell number between P6 and P8. In addition, as determined by the MTT assay, ASCs and dsASCs passage 2 cells exhibited similar proliferation rates for up to 72 hours (Figure 2C).

Immunophenotype of dsASCs

Passage 1 dsASCs (20,000 cells per well) were grown in two-well chamber slides for 24 to 48 hours and stained positive for stem cell specific surface markers Thy-1 (CD90) and Endoglin (CD105; Figure 3A, 3B). The dsASCs also stained positive for PDGFRβ⁺ (Figure 3C) and STRO-1⁺ (Figure 3D), suggesting that the cells isolated from the floating fraction of the debrided hypodermis originated from the perivascular space surrounding the adipocytes while maintaining their stem cell characteristics.

FACS analysis of P1 cells (Figure 3E–H) indicates that most of the cell population is a subset within the parent population and demonstrates a positive stem cell immunophenotype—CD90⁺, CD105⁺, STRO-1⁺. These results indicate that dsASCs isolated from the discarded skin of burn patients had equivalent percentages of a true stem cell population in consensus with ASCs isolated from adipose tissues obtained from a human abdominoplasty (data not shown).

Matrix-Directed dsASCs Differentiation

Using the inherent cues of matrix microenvironments (three-dimensional collagen hydrogels, PEGylated fibrin, and collagen-PEGylated fibrin bilayer composites), dsASCs differentiated into distinct phenotypic morphologies. Figure 4A–C shows cross-sectional images of the collagen, PEGylated fibrin, and collagen-PEGylated fibrin hydrogels. Passage 2 dsASCs (50,000 cells/ml) mixed with the collagen-based hydrogel exhibited spindle-shaped morphology by day 5 (Figure 4D) and populated the entire collagen hydrogel by day 10, maintaining fibroblast-like phenotype (Figure 4E). Within the PEGylated fibrin-based hydrogel, dsASCs began to exhibit cellular extensions by day 3 and formed prominent connections with other cells by day 5 (Figure 4F) and formed dense multicellular networks (Figure 4G) by day 10.

To mimic a vascularized dermal equivalent, a composite of PEGylated fibrin-collagen bilayer hydrogel was prepared using equal numbers of dsASCs within each hydrogel layer. When subjected to uniform culture condition, dsASCs simultaneously adapted a differential phenotype within the different hydrogel layers (Figure 4H–K). Analogous to morphological changes observed within individual hydrogel systems, dsASCs maintained their spindle-shaped morphology in the collagen matrix (Figure 4H and I)**,** or simultaneously differentiated into tubular networks (Figure 4J) in the PEGylated fibrin hydrogel matrix of the dsASCS-bilayer hydrogel construct. This experiment provides evidence that dsASCs may be optimal for developing either a vascular or a dermal composite individually or in combination for wound regeneration.

Influence of dsASCS-Bilayer Hydrogels on Full-Thickness Wound Healing

Rat excision wounds treated with PEGylated fibrin-collagen bilayer hydrogels showed decreased wound contraction over time with faster wound closure in comparison with saline-treated controls (Figure 5A). By day 16, wounds treated with the bilayer hydrogels alone and dsASCS-bilayer hydrogels showed no significant difference in healing, 94 to 95% wound closure, whereas saline-treated controls showed 79% wound closure (Figure 5B).

Histological analysis of the wound bed from saline-treated control animals showed little dermal matrix deposition and an absence of any re-epithelialization by day 8 (Figure 6A, 6B), and by day 16, the wound bed still had poor matrix remodeling and showed incomplete re-epithelialization (Figure 6C, 6D). Animals treated with bilayer hydrogels alone showed an increase in granulation tissue formation by day 8 (Figure 6E; serrated line across wound bed and Figure 6F) and by day 16 showed a significant re-epithelializing wound margin with minimal scab adhering to the wound bed (Figure 6G, 6H; bold arrow). In animals treated with the dsASCS-bilayer hydrogels there was integration of hydrogel matrix within the wound bed by day 8 (Figure 6I; serrated circle, Figure 6J), progression of epithelial margin toward the center of the wound (Figure 6I, bold arrows), and better dermal matrix deposition (Figure 6I, serrated line across wound bed). By day 16, the wounds showed complete re-epithelialization (Figure 6K, 6L; serrated line) and prominent remodeling of the dermal layer and the presence of well-defined dermal and epithelial layers (Figure 6L). Although both the hydrogel-treated groups showed comparably similar re-epithelialization, the groups treated with dsASCS-bilayer hydrogels showed less contraction when the wound bed areas were compared (between vertical serrated line in Figure 6G and 6K).

DISCUSSION

In recent years, it has been shown that ASCs derived from stromal vascular fraction have the capacity to be used in development of tissue-engineered constructs for various applications.[30,31] ASCs have been shown to reside at the pericytic region of microvessels,[32] and these spindle-shaped fibroblast-like cells have the propensity to differentiate into multiple cell phenotypes.[17,31] We recently showed that some of these resident stem cells in the perivascular regions are able to survive after burn trauma.[18] Furthermore,
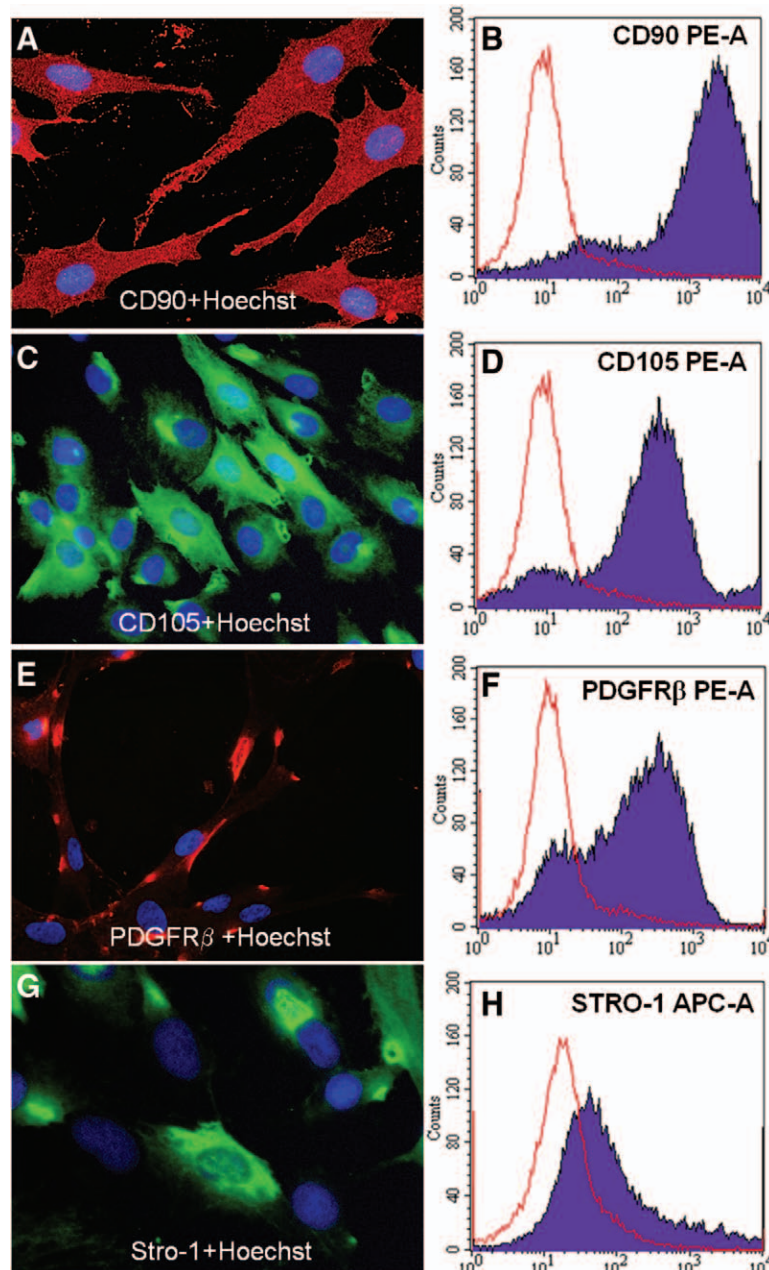

Figure 3. Immunocytochemical images of debrided skin adipose stem cells stained for various stem cell surface markers. A. CD90, (C) CD105, (E) PDGFRβ, and (G) STRO-1. Micrographs of cells fluorescently labeled with Alexa Fluor® 594 (A and E) or with Alexa Fluor® 488 (C and G). Original magnification: ×400. FACS histograms of different stem cell surface markers (B) CD90, (D) CD105, (F) PDGFRβ, and (H) STRO-1. For all FACS analysis, 20,000 events were collected (n = 2, percentage population ± SD) and analyzed for the total population positive for specific cell surface markers. The red line plot in all the FACS histograms represents isotype-matched antibody controls. *APC*, allophycocyanin; *PE*, phycoerythrin; *PDGFR*β, platelet-derived growth factor receptor beta; *FACS*, fluorescence-activated cell sorting.
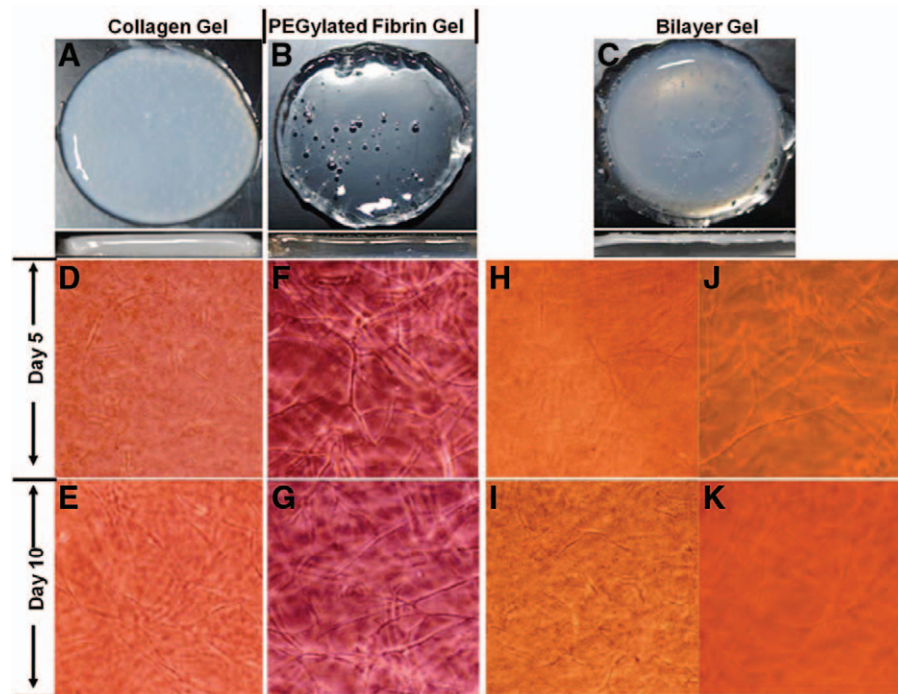
Figure 4. Photographic images of hydrogels, (A) collagen, (B) PEGylated fibrin, and (C) PEGylated fibrin-collagen bilayer. Inset at the bottom of each photograph shows their respective cross-sectional images. Light microscopic images depicting the differentiation time course of debrided skin adipose stem cells in (D, E) collagen, (F, G) PEGylated fibrin, and (H-K) PEGylated fibrin-collagen bilayer hydrogels. Bright field images original magnification: ×100. *PEGylated*, polyethylene gylated.

these stem cells dsASCs can be isolated from subcutaneous hypodermis of debrided burned skin through a similar process used to isolate ASCs from lipoaspirates.[33,34] Here, we show that dsASCs have a morphological appearance similar to that of ASCs isolated from adipose tissue obtained through abdominoplasty procedure. The patient population within this study included both male and female subjects of varying age groups, and the stem cells isolated from the patient population included in this study were morphologically similar within these categories to ASCs isolated from normal human lipoaspirates. From our previous study, we observed that there is no difference in total cell yields between the burned patients' ages[18] and that it is analogous to ASCs isolated from normal human lipoaspirates.[35] In this study, however, we show that the proliferation rate of dsASCs (P1–P7) is retarded in older patients after P4 compared with dsASCs isolated from younger patients. In addition, there was no significant difference in the cell proliferation rate between the ASCs from abdominoplasty and dsASCs from burned skin samples. This result suggests that a correlation between influences of resident stem cell self-renewal and patient age may exist during burn wound healing and the stem cells obtained from abdominoplasty tissue and burn skin samples behave similarly in terms of cell proliferation and function. Furthermore, dsASCs express a panel of immunophenotypic markers that are used to identify ASCs from normal uninjured tissue.[36] Although ASCs are a subpopulation that resides within a heterogeneous mixture of cells in the stromal vascular fraction from lipoaspirates, they can be culture-expanded as a clonal subset.[37] Similarly, more than 80% of P1 dsASCs are CD90^{+}, CD105^{+}, PDGFRβ^{+}, STRO-1^{+}, indicating the persistence of stem cells within the perivascualar niche of adipose tissue, even after burn trauma. These stem cells constitute a major source that can be used as a fresh isolate or in combination with an appropriate scaffold to develop a required tissue-engineered skin replacement product. In our present study, we have made use of two natural biomaterials widely used for clinical purposes—collagen and fibrin-based scaffolds.

Benefits of ASCs in combination with collagen-based matrices are investigated in both in vivo and in vitro systems.[38] When dsASCs are embedded within a collagen hydrogel scaffold, they are able to proliferate and maintain spindle-shaped morphology for 10 days, analogous to our previous observation.[39] Like collagen, fibrin has also been used for various biomedical applications. Fibrin
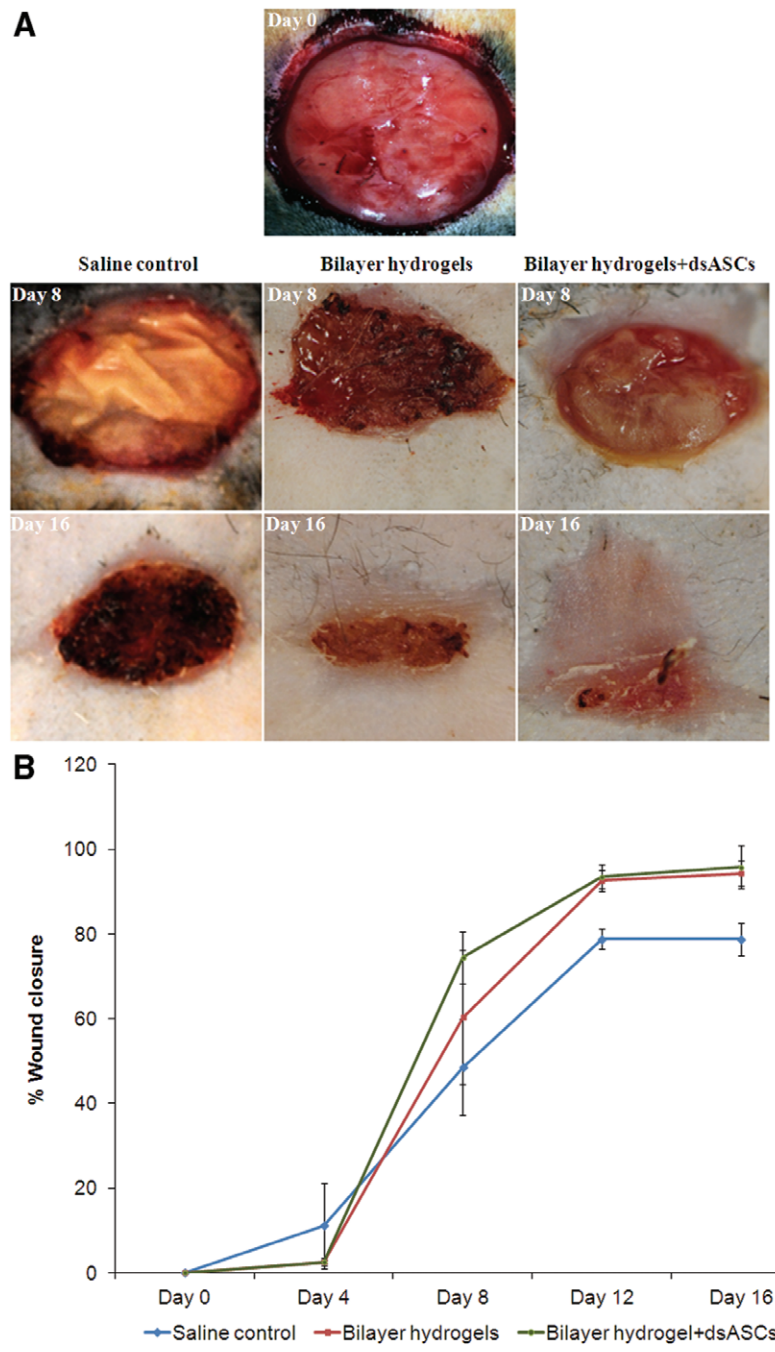
Figure 5. Excision wound closure observed in athymic rats. A. Photomicrograph images of wound at days 8 and 16. B. Graph showing the percentage wound closure observed over time in saline-treated control, polyethylene gylated fibrin-collagen bilayer hydrogel, and (Polyethylene gylated fibrin-collagen bilayer)–dsASCs hydrogel with wounds. *dsASCs*, debrided skin adipose stem cells.

gels are routinely used for clinical purposes because they promote hemostasis, wound healing, and tissue connection, and prevent infections.[40] Fibrin has been previously investigated as a delivery vehicle for preadipocyte cultures.[41] In addition, fibrin hydrogels have applications for promoting angiogenesis. Major disadvantages with fibrin as a potential scaffold are

low mechanical stiffness and its rapid degradation. To overcome these disadvantages, fibrin hydrogels are cross-linked with PEG. Additionally, it has been shown that PEGylated fibrin hydrogels promote mesenchymal stem cell differentiation into vascular phenotypes in vitro. Similarly, when dsASCs are embedded within PEGylated fibrin hydrogels, they
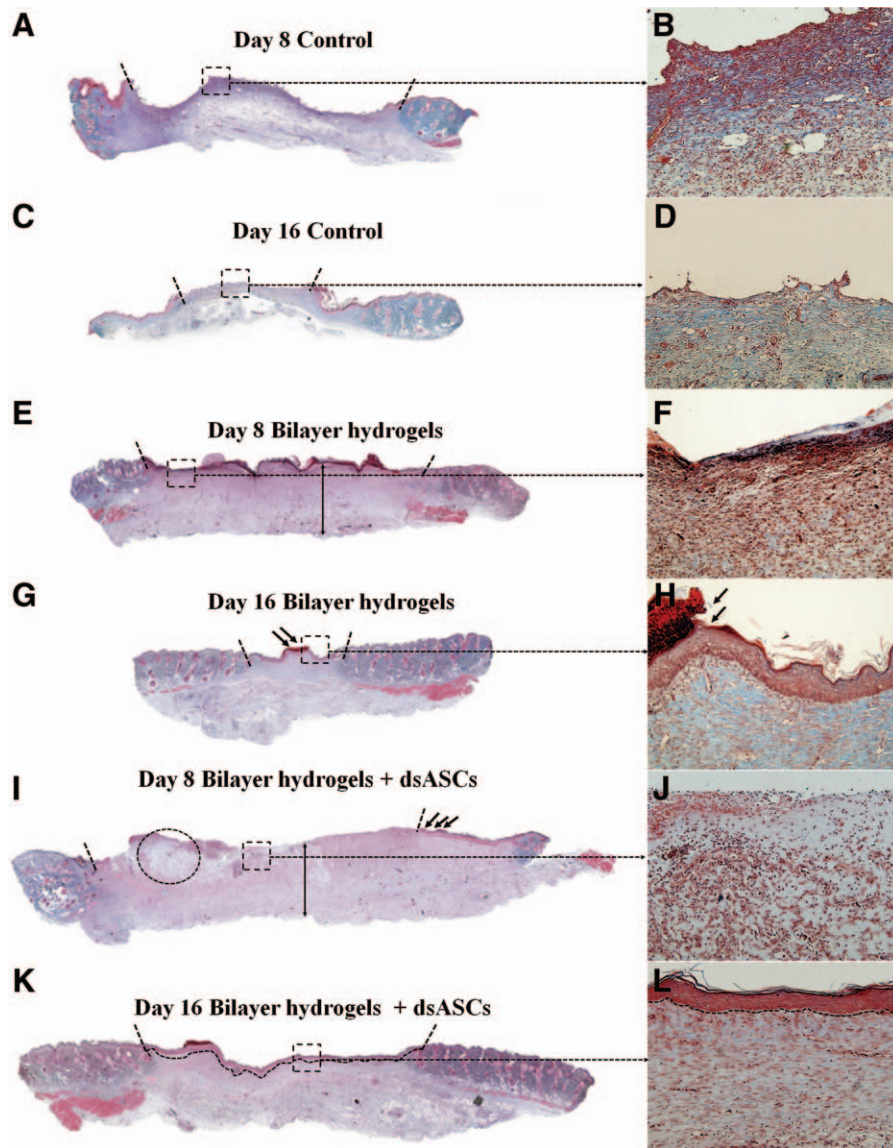
Figure 6. Masson trichrome stained tissue sections of excision wounds. A–D. Photomicrographs of saline control tissue sections taken from day 8 and day 16. E–H. Photomicrographs of tissue sections of wounds treated with PEGylated fibrin-collagen bilayer hydrogels. I–L. Photomicrographs of tissue sections of wounds treated with dsASCS-bilayer hydrogels. Serrated vertical line over photomicrographs (A, C, G, I, and K) represent the healing progression of the wound margin from the periphery of intact skin surface. Original magnification: ×40 (A, C, E, G, I, and K), ×100 (B, D, F, H, J, and L). *dsASCs*, debrided skin adipose stem cells.

exhibit a robust network formation in vitro. Recently, human ASCs differentiated into endothelial cells were seeded along with human fibroblasts into a porous collagen-based scaffold to obtain an endothelialized dermal equivalent. Previously, we prepared a bilayer hydrogel construct combining a collagen and PEGylated fibrin matrix with ASCs.[29] In the present study, we show that dsASCs, when seeded within a bilayer construct, can[42] form vascular network structures in the PEGylated fibrin hydrogel layer while maintaining a fibroblast-like morphology in the collagen layer. This phenomenon is solely dictated by the matrix microenvironment of both hydrogel types. Therefore, bilayer matrices can direct stem cell phenotypes as well as be a template for the creation of layered composites.

As the structural aspects of a bilayer scaffold regulate ASCs attachment and differentiation, we additionally investigated the regenerative ability of a dsASCs-bilayer hydrogel using an athymic rat full-thickness wound model. Bilayer hydrogels prepared in this study consisted of ≈ 3.5 cm^2 surface

area with 1×10^5 dsASCs in each hydrogel layer, which was sufficient to cover an acute wound with a total area of $\approx 1.8\,cm^2$. As an approximation, it is clinically scalable to be able to cover larger surface area wounds. Application of the bilayer hydrogel to a wound improved matrix deposition and enhanced the epithelial migration toward the center of the wound. Although there was no significant difference between the two bilayer hydrogel group in terms of re-epithlialization, the wounds treated with dsASCs-bilayer hydrogels showed less contraction. We have previously shown that dsASCs are able to integrate within a wound bed when topically applied.[18] Another study showed that a skin substitute implementing ASCs engrafted into wounds created in athymic mice and promoted epidermal regeneration and skin integrity in vivo.[15] Histological analysis of the wounds treated with bilayer hydrogels provide evidence for the presence of a well-defined dermis infiltrated with nascent collagen bundles. Further investigations are currently under way to determine the vascular density, localization of dsASCs within a wound bed, and the cellular phenotypes present. This preliminary investigation demonstrates that dsASCs may contribute significantly to wound healing and skin regeneration either directly or via paracrine signaling. This analysis will provide mechanistic insight on the contribution of the dsASCs-bilayer construct to wound healing and skin regeneration.

In summary, it is our goal to develop a layered composite wound dressing or vascularized dermal equivalent for severe trauma cases in which accessibility of normal tissue sources is clinically complicated. The bilayer hydrogel scaffold seeded with autologous stem cell (dsASCs) derived from debrided burned tissue provides a viable option for treating these complicated wounds. It is a practical approach to isolate stem cells from discarded burned tissue in consistent quantities to cover large surface areas in combination with clinically approved biomaterials. Considering that extensive burn wounds require extensive debridement, this "waste tissue" represents an invaluable stem cell repository to develop tissue-engineered constructs. Promising in vitro and in vivo results presented here provide support for the use of dsASCs-bilayer hydrogels to treat large surface area wounds.

ACKNOWLEDGMENTS

REFERENCES

1. Chung KK, Blackbourne LH, Wolf SE, et al. Evolution of burn resuscitation in operation Iraqi freedom. J Burn Care Res 2006;27:606–11.
2. White CE, Renz EM. Advances in surgical care: management of severe burn injury. Crit Care Med 2008;36(7 Suppl):S318–24.
3. Wolf SE, Kauvar DS, Wade CE, et al. Comparison between civilian burns and combat burns from Operation Iraqi Freedom and Operation Enduring Freedom. Ann Surg 2006;243:786–92; discussion 792–5.
4. Bremner LF, Mazurek M. Reconstructive challenges of complex battlefield injury. J Surg Orthop Adv 2010;19:77–84.
5. Owens BD, Wenke JC, Svoboda SJ, White DW. Extremity trauma research in the United States Army. J Am Acad Orthop Surg 2006;14(10 Spec No.):S37–40.
6. Kauvar DS, Cancio LC, Wolf SE, Wade CE, Holcomb JB. Comparison of combat and non-combat burns from ongoing U.S. military operations. J Surg Res 2006;132:195–200.
7. Ehrenreich M, Ruszczak Z. Tissue-engineered temporary wound coverings. Important options for the clinician. Acta Dermatovenerol Alp Panonica Adriat 2006;15:5–13.
8. Ehrenreich M, Ruszczak Z. Update on tissue-engineered biological dressings. Tissue Eng 2006;12:2407–24.
9. Metcalfe AD, Ferguson MW. Tissue engineering of replacement skin: the crossroads of biomaterials, wound healing, embryonic development, stem cells and regeneration. J R Soc Interface 2007;4:413–37.
10. Boyce ST. Cultured skin substitutes: a review. Tissue Eng 1996;2:255–66.
11. Badiavas EV, Abedi M, Butmarc J, Falanga V, Quesenberry P. Participation of bone marrow derived cells in cutaneous wound healing. J Cell Physiol 2003;196:245–50.
12. Kataoka K, Medina RJ, Kageyama T, et al. Participation of adult mouse bone marrow cells in reconstitution of skin. Am J Pathol 2003;163:1227–31.
13. Cherubino M, Rubin JP, Miljkovic N, Kelmendi-Doko A, Marra KG. Adipose-derived stem cells for wound healing applications. Ann Plast Surg 2011;66:210–5.
14. Jeong JH. Adipose stem cells and skin repair. Curr Stem Cell Res Ther 2010;5:137–40.
15. Trottier V, Marceau-Fortier G, Germain L, Vincent C, Fradette J. IFATS collection: Using human adipose-derived stem/stromal cells for the production of new skin substitutes. Stem Cells 2008;26:2713–23.
16. Aust L, Devlin B, Foster SJ, et al. Yield of human adipose-derived adult stem cells from liposuction aspirates. Cytotherapy 2004;6:7–14.
17. Prunet-Marcassus B, Cousin B, Caton D, André M, Pénicaud L, Casteilla L. From heterogeneity to plasticity in adipose tissues: site-specific differences. Exp Cell Res 2006;312:727–36.
18. Natesan S, Wrice NL, Baer DG, Christy RJ. Debrided skin as a source of autologous stem cells for wound repair. Stem Cells 2011;29:1219–30.
19. Lutolf MP, Gilbert PM, Blau HM. Designing materials to direct stem-cell fate. Nature 2009;462:433–41.
20. Metcalfe AD, Ferguson MW. Bioengineering skin using mechanisms of regeneration and repair. Biomaterials 2007;28:5100–13.

21. Pennesi G, Scaglione S, Giannoni P, Quarto R. Regulatory influence of scaffolds on cell behavior: how cells decode biomaterials. Curr Pharm Biotechnol 2011;12:151–9.

22. Votteler M, Kluger PJ, Walles H, Schenke-Layland K. Stem cell microenvironments–unveiling the secret of how stem cell fate is defined. Macromol Biosci 2010;10:1302–15.

23. Girandon L, Kregar-Velikonja N, Božikov K, Barli A. In vitro models for adipose tissue engineering with adipose-derived stem cells using different scaffolds of natural origin. Folia Biol (Praha) 2011;57:47–56.

24. Liu S, Zhang H, Zhang X, et al. Synergistic angiogenesis promoting effects of extracellular matrix scaffolds and adipose-derived stem cells during wound repair. Tissue Eng Part A 2011;17:725–39.

25. Nambu M, Ishihara M, Kishimoto S, et al. Stimulatory effect of autologous adipose tissue-derived stromal cells in an atelocollagen matrix on wound healing in diabetic db/db mice. J Tissue Eng 2011;2011:158105.

26. Mosmann T. Rapid colorimetric assay for cellular growth and survival: application to proliferation and cytotoxicity assays. J Immunol Methods 1983;65:55–63.

27. Zhang G, Drinnan CT, Geuss LR, Suggs LJ. Vascular differentiation of bone marrow stem cells is directed by a tunable three-dimensional matrix. Acta Biomater 2010;6:3395–403.

28. Zhang G, Wang X, Wang Z, Zhang J, Suggs L. A PEGylated fibrin patch for mesenchymal stem cell delivery. Tissue Eng 2006;12:9–19.

29. Natesan S, Zhang G, Baer DG, Walters TJ, Christy RJ, Suggs LJ. A bilayer construct controls adipose-derived stem cell differentiation into endothelial cells and pericytes without growth factor stimulation. Tissue Eng Part A 2011;17:941–53.

30. Zuk PA, Zhu M, Ashjian P, et al. Human adipose tissue is a source of multipotent stem cells. Mol Biol Cell 2002;13:4279–95.

31. Zuk PA, Zhu M, Mizuno H, et al. Multilineage cells from human adipose tissue: implications for cell-based therapies. Tissue Eng 2001;7:211–28.

32. Traktuev DO, Merfeld-Clauss S, Li J, et al. A population of multipotent CD34-positive adipose stromal cells share pericyte and mesenchymal surface markers, reside in a periendothelial location, and stabilize endothelial networks. Circ Res 2008;102:77–85.

33. Gronthos S, Franklin DM, Leddy HA, Robey PG, Storms RW, Gimble JM. Surface protein characterization of human adipose tissue-derived stromal cells. J Cell Physiol 2001;189:54–63.

34. Varma MJ, Breuls RG, Schouten TE, et al. Phenotypical and functional characterization of freshly isolated adipose tissue-derived stem cells. Stem Cells Dev 2007;16:91–104.

35. Mojallal A, Lequeux C, Shipkov C, et al. Influence of age and body mass index on the yield and proliferation capacity of adipose-derived stem cells. Aesthetic Plast Surg 2011;35:1097–105.

36. Mitchell JB, McIntosh K, Zvonic S, et al. Immunophenotype of human adipose-derived cells: temporal changes in stromal-associated and stem cell-associated markers. Stem Cells 2006;24:376–85.

37. Yoshimura K, Shigeura T, Matsumoto D, et al. Characterization of freshly isolated and cultured cells derived from the fatty and fluid portions of liposuction aspirates. J Cell Physiol 2006;208:64–76.

38. Orbay H, Takami Y, Hyakusoku H, Mizuno H. Acellular dermal matrix seeded with adipose-derived stem cells as a subcutaneous implant. Aesthetic Plast Surg 2011;35:756–63.

39. Natesan S, Baer DG, Walters TJ, Babu M, Christy RJ. Adipose-derived stem cell delivery into collagen gels using chitosan microspheres. Tissue Eng Part A 2010;16:1369–84.

40. Janmey PA, Winer JP, Weisel JW. Fibrin gels and their clinical and bioengineering applications. J R Soc Interface 2009;6:1–10.

41. Schoeller T, Lille S, Wechselberger G, et al. Histomorphologic and volumetric analysis of implanted autologous preadipocyte cultures suspended in fibrin glue: a potential new source for tissue augmentation. Aesthetic Plast Surg 2001;25:57–63.

42. Auxenfans C, Lequeux C, Perrusel E, Mojallal A, Kinikoglu B, Damour O. Adipose-derived stem cells (ASCs) as a source of endothelial cells in the reconstruction of endothelialized skin equivalents. J Tissue Eng Regen Med 2012;6:512–8.